Dielectric Properties Determination of a Stratified Medium

Paiboon YOIYOD, Monai KRAIRIKSH

Faculty of Engineering, King Mongkut's Institute of Technology Ladkrabang, Bangkok 10520, Thailand

S3610116@kmitl.ac.th, kkmonai@kmitl.ac.th

Abstract. *The method of detection of variation in dielectric properties of a material covered with another material, which requires nondestructive measurement, has numerous applications and the accurate measurement system is desirable. This paper presents a dielectric properties determination technique whereby the dielectric constant and loss factor are extracted from the measured reflection coefficient. The high frequency reflection coefficient shows the effect of the upper layer, while the dielectric properties of the lower layer can be determined at the lower frequency. The proposed technique is illustrated in 1-11 GHz band using 5 mm-thick water and 5% saline solution. The fluctuation of the dielectric properties between the high frequency and the low frequency, results from the edge diffraction in the material and the multiple reflections at the boundary of the two media, are invalid results. With the proposed technique, the dielectric properties of the lower layer can be accurately determined. The system is validated by measurement and good agreement is obtained at the frequency below 3.5 GHz. It can be applied for justifying variation of the material in the lower layer which is important in industrial process.*

Keywords

Dielectric properties, stratified medium, reflection coefficient, diffraction coefficient

1. Introduction

The dielectric properties determination of a covered material or stratified medium by using a microwave technique is essential and has numerous applications. One of the determination techniques of dielectric properties is the free space technique whose main advantages include distinguishing capability of inhomogeneous materials, nondestructiveness, non-contact, and no machinery that fits the sample required despite sophisticated procedure to obtain accurate results [1], [2]. The techniques need an insertion of a perfectly conducting plate behind the plate of unknown material. The comprehensive reviews of dielectric properties measurement techniques and nondestructive testing using both millimeter and microwave are respectively shown in [3]. Such measurement techniques together with nondestructive testing are employed in a number of applications, such as moisture content detection [4–6], determination of liquids [7], skin cancer detection [8], surface crack detection [9], corrosion detection [10], [11], in which some sensors require contact [7–11] while the other are contactless [5], [6]. Apart from the contactless measurement, certain techniques require embedding of a scatterer in the medium under test [12], [13] which inevitably results in limitation in some applications as in agricultural applications [14], [15].

The work in [16] utilized a free space technique to characterize ripeness of mango but sample of mango must be prepared in a planar sample holder. Therefore, it is unsuitable in practice. A number of the free space techniques widely employed in the past, the sole magnitude measurement technique is less complex and thus inexpensive; nevertheless, it requires transmission measurement [17]. In addition, the use of millimeter wave reflectometer [18] is one of the attractive solutions. Fruit testing nevertheless must be carried out by measuring through the peel nondestructively. The methods in [19], [20] estimate the dielectric properties and thickness of multilayer object but they are contact measurement. The contactless measurement can however be accomplished by the technique of through-wall measurement [21]. From the aforementioned statement, it is desirable to estimate dielectric properties of a stratified object, consisting of the upper layer, lower layer, and the thickness of the upper layer. The issue is that the low variation of dielectric properties of the lower layer has little effect on the total variation of the measured results. Therefore, it is necessary to propose an accurate measurement technique to estimate the dielectric properties and thickness of the upper layer, which leads to the accurate estimation of the dielectric properties of the lower layer.

To develop a measurement system, a measurement technique for determination of not merely the dielectric properties of upper and lower layers but also the thickness of upper layer must be well established. To this end, in this paper the reflection measurement in wideband to determine the dielectric properties of the upper layer with high frequencies in which depth of penetration is shorter than the depth of the upper layer is introduced. The measured material is supposed to be in a data base for comparing dielectric properties of the upper layer when measured at high

frequency, and then the values at the lower frequency can be obtained. The application of interest is measurement of material in a container in industrial process. The relevant work is the reflection measurement for estimating thickness of snow on the road [22]. Using the full band dielectric properties, it is possible to calculate depth of penetration of wave through the upper layer and thus velocity of wave in the upper layer. As a result, the thickness of the upper layer is determined. The suitable frequency at the lower frequency band is selected from the frequency response of the dielectric properties. Finally, the dielectric properties of the lower layer can be determined. To obtain a tangible insight into the aforesaid technique, the planar structure is investigated in this paper.

The organization of this paper begins with the introduction in Sec. 1. Section 2 discusses the principles of the proposed technique. The calculation results of the measurement technique are illustrated in Sec. 3. Validation of the calculation results, together with the discussions, is carried out by measurements shown in Sec. 4. Section 5 discusses the limitation of the system and addresses the factors affecting the required bandwidth. This paper is then ended with a conclusion in Sec. 6.

2. Dielectric Properties Determination of a Stratified Medium

Let us consider a stratified medium of planar structure with upper layer thickness d as shown in Fig. 1. The upper medium has dielectric properties of μ_1, ε_1 and σ_1. The lower layer is infinite extent in thickness and possesses dielectric properties of μ_2, ε_2 and σ_2. The width and length of the structure are finite size with the width of W. This structure is illuminated by a uniform plane wave in free space in which dielectric properties are μ_0, ε_0 and σ_0, where σ_0 is zero. Fig. 1 depicts the various components of waves for derivation of the reflection coefficient. The transmitting and receiving antennas are at *O(x',y',z')* and *P(x,y,z)*, respectively, where position of y' is same as y at $W/2$, *O(x',y',z')* and *P(x,y,z)* are almost identical position to act as a monostatic radar. The transmitter transmits incident electric wave E_i on the upper surface at $z = -d$. With perfect isolation between the two antennas, the receiving antenna receives reflected and diffracted waves from four edges (D_1, D_2, D_3 and D_4). The reflected wave is the sum of the reflection at the upper surface and the multiple reflections between the upper surface and the interface between dielectric 1 and dielectric 2. The reflection coefficient at $z = -d$ ($\Gamma_{in}(z = -d)$) can be expressed as (1).

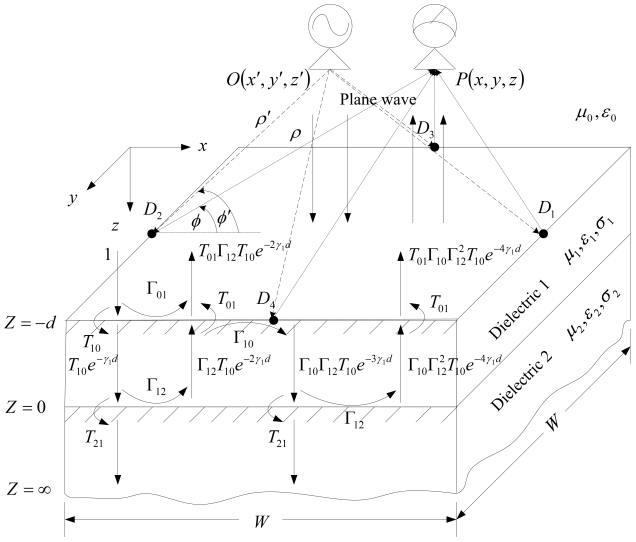

Fig. 1. Geometry of the problem.

$$\Gamma_{in}(z=-d)=\Gamma_{01}+T_{01}T_{10}\sum_{i=1}^{n}\Gamma_{12}^{i}\Gamma_{10}^{i-1}e^{-2i\gamma_1 d}+D \tag{1}$$

where Γ_{01} and Γ_{10} are the reflection coefficients between the free space and the upper layer for propagation in upward direction and downward direction, respectively, T_{01} and T_{10} are the transmission coefficients between the free space and the upper layer for propagation in upward direction and downward direction, respectively, Γ_{12} is the reflection coefficient at the boundary of the two media, γ_1 is propagation constant in dielectric 1 ($\gamma_1 = \alpha_1 + j\beta_1$), i represents the i^{th} reflection, n is the number of multiple reflections in the material, and D is diffraction coefficient as shown in (2).

$$D=\frac{E_{D_1}+E_{D_2}+E_{D_3}+E_{D_4}}{E_i}. \tag{2}$$

Diffracted electric field intensity on each side from [23] is expressed in rectangular coordinate as follows

$$E_{D_k}(x,y,z)=\pm E_i\left\{T\left(\sqrt{\varepsilon_{r1}}\sin\left(\tan^{-1}\left(\frac{z}{x}\right)\right)-\sqrt{\varepsilon_{r1}-\cos^2\left(\tan^{-1}\left(\frac{z'}{x'}\right)\right)}\right)\right.$$
$$F_t\left(2k_d\left(\sqrt{(x^2+z^2)}\right)\cos^2\left(\frac{\tan^{-1}\left(\frac{z}{x}\right)-\cos^{-1}\left(\frac{\cos\left(\tan^{-1}\left(\frac{z'}{x'}\right)\right)}{\sqrt{\varepsilon_{r1}}}\right)}{2}\right)\right)$$
$$\times\frac{e^{-j\frac{\pi}{4}}}{2\sqrt{2\pi k_d}}\frac{}{\sqrt{\varepsilon_{r1}}\cos\left(\tan^{-1}\left(\frac{z}{x}\right)\right)+\cos\left(\tan^{-1}\left(\frac{z'}{x'}\right)\right)}$$
$$+T\left((1-R)\cos\left(\tan^{-1}\left(\frac{z'}{x'}\right)\right)-(1+R)\sqrt{\varepsilon_{r1}}\cos\left(\tan^{-1}\left(\frac{z}{x}\right)\right)\right)\frac{e^{-j\frac{\pi}{4}}}{2\sqrt{2\pi k_d}}$$
$$\left.\times\frac{F_t\left(2k_d\left(\sqrt{(x^2+z^2)}\right)\cos^2\left(\frac{\cos^{-1}\left(\sqrt{1-\frac{\cos^2\left(\tan^{-1}(z'/x')\right)}{\varepsilon_{r1}}}\right)-\left(\tan^{-1}\left(\frac{z}{x}\right)-\frac{\pi}{2}\right)}{2}\right)\right)}{\sqrt{\varepsilon_{r1}}\cos\left(\tan^{-1}\left(\frac{z}{x}\right)+\frac{\pi}{2}\right)-\sqrt{\varepsilon_{r1}-\cos^2\left(\tan^{-1}\left(\frac{z'}{x'}\right)\right)}}\right\} \tag{3}$$

where E_i is the incident electric field intensity, T and R are Fresnel transmission coefficient and reflection coefficient, respectively, k = 1, 2, 3 and 4 for electric field intensity on each side, (+) is for perpendicular polarized and (-) is for parallel polarized diffraction coefficients. ρ is a distance from the diffraction point to the observation point $\rho = (x^2 + z^2)^{1/2}$, ϕ is an angle between the line from the diffraction point to the observation point with respect to x-axis $\phi = \tan^{-1}(z/x)$, ρ' is a distance from source point to diffraction point $\rho' = (x'^2 + z'^2)^{1/2}$, ϕ' is an angle between the line from the source point to the diffraction point with respect to x-axis $\phi' = \tan^{-1}(z'/x')$, and ε_{r1} is relative permittivity of dielectric 1.

Since every reflection and transmission term in the summation has a very low magnitude, therefore the summation shrinks very rapidly. Hence, the summation in (1) can be truncated as shown in (4a).

$$\Gamma_{in} = \Gamma_{01} + \frac{T_{01}T_{10}\Gamma_{12}e^{-2\gamma_1 d}}{1-\Gamma_{10}\Gamma_{12}e^{-2\gamma_1 d}} + D \tag{4a}$$

where $\Gamma_{10} = -\Gamma_{01}$, $T_{10} = 1 + \Gamma_{01}$ and $T_{01} = 1 + \Gamma_{10} = 1 - \Gamma_{01}$. Hence

$$\Gamma_{in} = \frac{\Gamma_{01} + \Gamma_{12}e^{-2\gamma_1 d}}{1+\Gamma_{01}\Gamma_{12}e^{-2\gamma_1 d}} + D. \tag{4b}$$

Rewriting (4b), one can solve for Γ_{12} as shown in (5). In order to get d, we use the reflection coefficient in time domain. The detail is explained in Sec. 3.1.

$$\Gamma_{12} = \frac{\Gamma_{in} - \Gamma_{01} - D}{(1-\Gamma_{01}(\Gamma_{in} - D))e^{-2\alpha_1 d}e^{-j2\beta_1 d}}. \tag{5}$$

α_1 and β_1 are respectively the attenuation constant and phase constant in the upper medium. For very high frequencies, attenuation through the upper layer is great enough such that $\Gamma_{in} \approx \Gamma_{01}$. The intrinsic impedance of the upper layer, η_1, can be directly calculated and then curve fitted to the database of the material to estimate η_1 values for lower frequencies. Using η_1 to characterize other parameters including η_2, the intrinsic impedance of the lower layer derived from (5), can be solved.

$$\eta_2 = \frac{\eta_1[(\Gamma_{in} - \Gamma_{01}) + (1-\Gamma_{in}\Gamma_{01})e^{-2\alpha_1 d}e^{-j2\beta_1 d}]}{(1-\Gamma_{in}\Gamma_{01})e^{-2\alpha_1 d}e^{-j2\beta_1 d} - (\Gamma_{in} - \Gamma_{01})} \tag{6}$$

or

$$\frac{\sigma_2 + j\omega\varepsilon_2}{j\omega\mu_2} = \frac{1}{\left[\dfrac{\eta_1[(\Gamma_{in} - \Gamma_{01}) + (1-\Gamma_{in}\Gamma_{01})e^{-2\alpha_1 d}e^{-j2\beta_1 d}]}{(1-\Gamma_{in}\Gamma_{01})e^{-2\alpha_1 d}e^{-j2\beta_1 d} - (\Gamma_{in} - \Gamma_{01})}\right]^2} \tag{7}$$

where $\eta_2 = x + jy$. Hence

$$\frac{\varepsilon_0\varepsilon''_{r2}}{j\mu_0\mu_{r2}} + \frac{\varepsilon_0(\varepsilon'_{r2} - j\varepsilon''_{r2})}{\mu_0\mu_{r2}} = \frac{1}{(x+jy)^2} \tag{8}$$

and

$$\frac{\varepsilon_0\varepsilon'_{r2}}{\mu_0\mu_{r2}} - j\frac{2\varepsilon_0\varepsilon''_{r2}}{\mu_0\mu_{r2}} = \frac{x^2 - y^2 - j2xy}{(x^2-y^2)^2 + (2xy)^2}. \tag{9}$$

By equating the real part of the left hand side to that of the right hand side of (9), and the imaginary part is also equated in the same manner, the dielectric properties can be derived from the real part x and imaginary part y of η_2

$$\frac{\varepsilon_0\varepsilon'_{r2}}{\mu_0\mu_{r2}} = \frac{x^2 - y^2}{(x^2-y^2)^2 + (2xy)^2}, \tag{10}$$

$$\frac{2\varepsilon_0\varepsilon''_{r2}}{\mu_0\mu_{r2}} = \frac{2xy}{(x^2-y^2)^2 + (2xy)^2}. \tag{11}$$

The dielectric constant and loss factor of the lower layer are expressed in a closed form as shown in (12) and (13), respectively.

$$\varepsilon'_{r2} = \frac{\mu_0\mu_{r2}(x^2 - y^2)}{\varepsilon_0((x^2-y^2)^2 + (2xy)^2)}, \tag{12}$$

$$\varepsilon''_{r2} = \frac{\mu_0\mu_{r2}(2xy)}{2\varepsilon_0((x^2-y^2)^2 + (2xy)^2)}. \tag{13}$$

From the above expressions, it can be seen that by measuring the reflection coefficient (Γ_{in}) at the upper surface in a wideband, the reflection coefficient between the free space and the upper layer (Γ_{01}) can be found from the high frequency which is unable to penetrate to the lower layer. Then, the dielectric properties of the upper layer at low frequency can be determined from the database. The above procedure is shown in a block diagram in Fig. 2.

Using the full band dielectric properties, it is possible to calculate the depth of penetration through the upper layer and consequently velocity of wave in the upper layer. From the result of reflection coefficient, the thickness d of the upper layer is determined by inverse Fourier transform

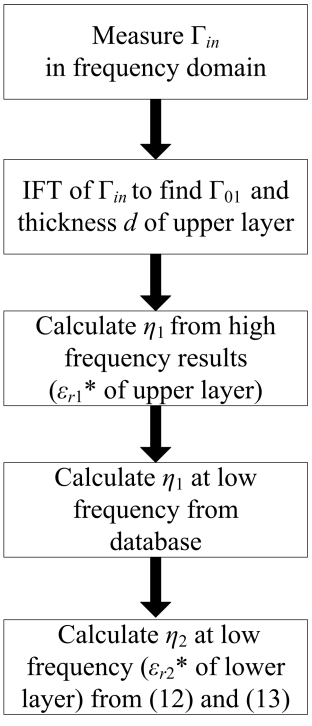

Fig. 2. Block diagram of the proposed technique.

(IFT). Using the high frequency for determining $\varepsilon_{r1}^* = \varepsilon_{r1}' - j\varepsilon_{r1}''$), then η_1 at low frequency is determined from the database of the material. Finally, the dielectric properties $\varepsilon_{r2}^* = \varepsilon_{r2}' - j\varepsilon_{r2}''$ of the lower layer η_2 are determined. This principle can be illustrated in Sec. 3.

3. Calculation Results

3.1 Determination of Thickness of the Upper Layer

At high frequency, the intrinsic impedance of the upper layer is calculated from (14)

$$\eta_1 = \eta_0 \left(\frac{1+\Gamma_{in}}{1-\Gamma_{in}} \right). \tag{14}$$

From the obtained dielectric properties at the high frequency band, the full band one can be obtained from the database of the material. For illustration, the material size of 18λ for the frequency of 6 GHz, the upper and lower layers are water and 5% saline solution [24], respectively. The resultant dielectric properties and depth of penetration of water and 5% saline solution are listed in Tab. 1.

Fig. 3(a) depicts the magnitude of reflection coefficient in frequency domain which was calculated using (4). The magnitude of reflection coefficient varies in a similar manner to damped sinusoidal below 5.5 GHz due to the effect of reflection at the upper surface and at the interface of the materials. Then, the steady response can be observed between 5.5 and 8.5 GHz since reflection takes place only at the upper surface. Note that the fluctuation at frequency higher than 8.5 GHz is caused by diffraction at the four edges of the material.

An inverse Fourier transforms of Γ_{in} provides the time-domain reflectometry as in Fig. 3(b). The first peak at 0 ns represents the reflection at the upper surface whereas the other peaks of the response represent the reflection between the upper and lower layers. Observing the time t, these peaks occur and accounting for the velocity of wave in the upper layer, a thickness of the upper layer can be determined from

Freq. (GHz)	Water	dp (mm)	5% saline	dp (mm)
1	77.960-j3.969	106	63.164-j141.956	3.51
2	77.230-j7.738	27	62.611-j75.443	2.83
3	76.144-j11.323	12	61.789-j55.085	2.46
4	74.741-j14.963	7.05	60.727-j46.141	2.14
5	73.066-j17.820	4.61	59.455-j41.464	1.86
6	71.164-j20.682	3.28	58.008-j39.268	1.62
7	69.082-j23.267	2.47	56.419-j38.006	1.42
8	66.866-j25.569	1.94	54.722-j37.358	1.24
9	64.588-j27.592	1.58	52.949-j37.051	1.1
10	62.196-j29.344	1.32	51.128-j36.923	0.98
11	59.814-j30.838	1.12	49.285-j36.879	0.88

Tab. 1. Dielectric properties and depth of penetration of water and 5% saline solution.

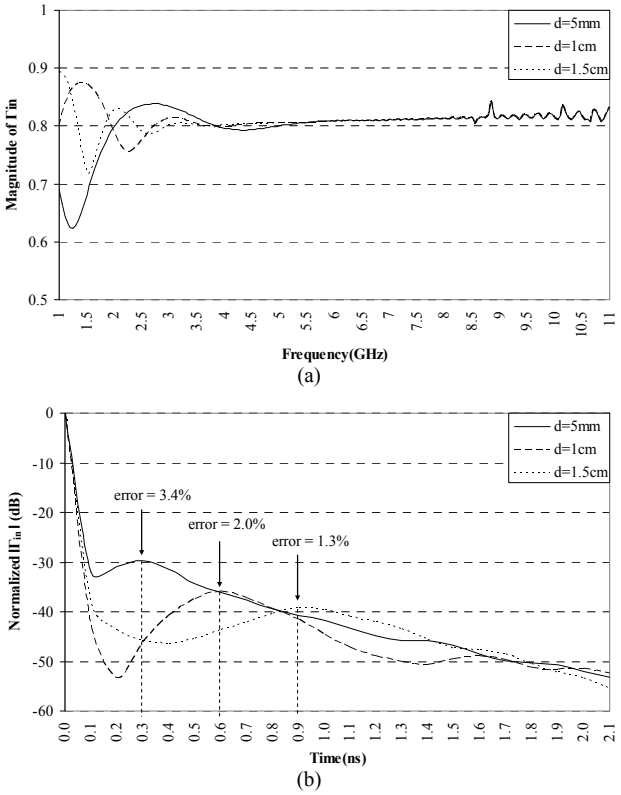

Fig. 3. Magnitude of reflection coefficient: (a) Frequency domain, (b) Time domain.

$$d = v_1 \cdot \frac{t}{2} \tag{15}$$

where v_1 is velocity of wave in the upper layer calculated from $v_1 = 1/(\mu\varepsilon_1)^{1/2}$ and t is the total time wave traveling forth and back. This velocity is obtained from the dielectric properties of water at the frequency corresponding to the time the peaks occur (at $f = 1/t$; dielectric properties of water are $75.754 - j12.358$, $77.488 - j6.625$ and $77.895 - j4.417$). v_1 at these frequencies are 0.344×10^8 m/s, 0.341×10^8 m/s and 0.340×10^8 m/s.

The estimated thickness for 5 mm, 1 cm and 1.5 cm layers are 5.15 mm (error 3.4%), 1.02 cm (error 2.0%) and 1.52 cm (error 1.3%), respectively. From Tab. 1, for the thickness of the upper layer of 5 mm, the frequencies lower than 5 GHz can penetrate to the lower layer. One can hence determine the dielectric properties of the lower layer. From the above results, it can be concluded that for the unknown upper and lower media, one can not only determine the dielectric properties and thickness of the upper layer by wideband measurement with the resulting thickness taken from inversed Fourier transform to time domain response, but also determine dielectric properties of the lower layer from the lower frequency.

With the above procedure, the different materials were investigated. It was found that when the upper and lower layers were respectively 5% saline solution and water, the frequency range for wideband measurement decreased since saline solution is lossier than water.

3.2 Dielectric Properties of Material with Different Dimensions

In practice, the size of the material is finite. Therefore, the effect of size contributes to the reflection coefficient and dielectric properties. In this regard, the size of the material was varied; the upper and lower layers are water (d = 5 mm) and 5% saline solution, respectively. Fig. 4 shows the determined dielectric properties of the material of interest with the size of 18λ and 42λ for the frequency of 6 GHz. Note that the fluctuations of the determined dielectric properties between 4.5-10.5 GHz are due to the edge diffraction in the material and the multiple reflection at the boundary of the two media that affect calculation of dielectric properties. The dielectric properties in this frequency band are invalid results. Those above 10.5 GHz are the dielectric properties of the upper layer whereas those below 4.5 GHz are for the lower layer. For the size of the material of 18λ and 42λ, the similar determined dielectric properties are obtained. The dielectric properties of material are not significantly affected by the size of the material. For dielectric constant in Fig. 4(a), the dielectric constant below 4.5 GHz approaches the dielectric constant of 5% saline solution and the one above 10.5 GHz approaches the dielectric constant of water. For loss factor, the frequency below 5 GHz approaches that of 5% saline solution and the one above 10.5 GHz approaches that of water as seen in Fig. 4(b).

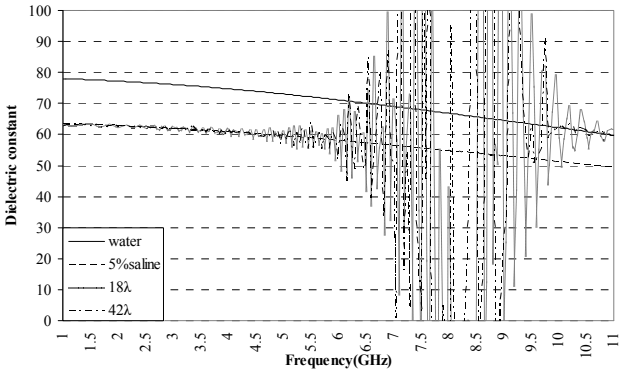

(a)

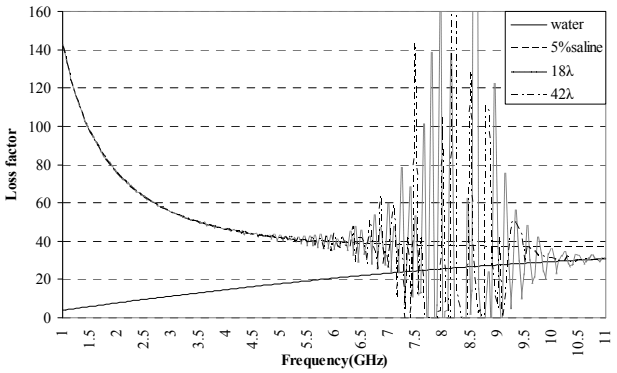

(b)

Fig. 4. Dielectric properties for different material dimensions (d = 5 mm, W = 18λ, 42λ at 6 GHz): (a) Dielectric constant, (b) Loss factor.

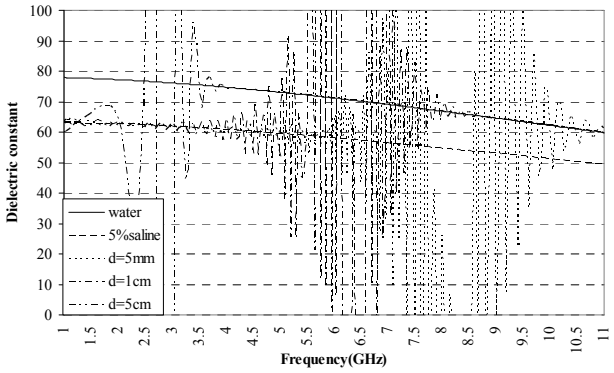

(a)

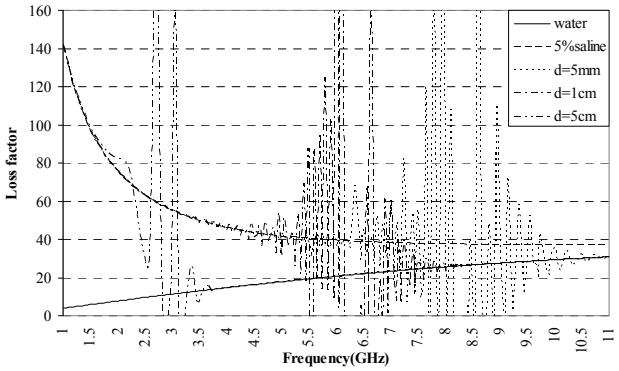

(b)

Fig. 5. Dielectric properties for different thickness of the upper layer (W = 18λ at 6 GHz): (a) Dielectric constant, (b) Loss factor.

Let us consider the variation of dielectric properties for various thicknesses of the upper layer of water, lower layer of 5% saline solution and material size of 18λ at 6 GHz, respectively. Fig. 5(a) shows variation of dielectric constant whereas Fig. 5 (b) shows variation of loss factor; for d equal to 5 mm, 1 cm and 5 cm. Obviously, the obtained dielectric properties of material depends on the thickness of the upper layer. The thin layer has a wide range of low frequency of the lower layer. On the other hand, the thick layer has a wide range of high frequency of the upper layer. The transition between the low and the high frequency responses has fluctuation which is related to thickness of the upper layer. Consider Fig. 5(a) the values of dielectric constant of 5% saline solution are obtained below 5 GHz (d = 5 mm), 3.5 GHz (d = 1 cm) and 1.25 GHz (d = 5 cm). On the other hand, the values of water are obtained above 10.5 GHz (d = 5 mm), 8 GHz (d = 1 cm) and 4 GHz (d = 5 cm), respectively. In Fig. 5(b), the values of loss factor of 5% saline solution are obtained below 5.5 GHz (d = 5 mm), 4.25 GHz (d = 1 cm) and 1.75 GHz (d = 5 cm). The values of water are obtained above 10.5 GHz (d = 5 mm), 8 GHz (d = 1 cm) and 3.75 GHz (d = 5 cm), respectively. It should be pointed out that the thickness of the upper layer has significant effect on frequency range of determined dielectric properties.

3.3 Variation of Dielectric Properties of the Lower Layer

In this illustration, the upper layer is water (d = 5 mm) and the material size is 18λ for the frequency of 6 GHz. When the material of the lower layer is changed from 5% to 15% saline solution, the frequency response is in the same fashion. From Fig. 6, the saline solution with higher concentration possesses lower dielectric constant and higher loss factor. Clearly, we can determine the variation of dielectric properties of the lower layer from the proposed technique.

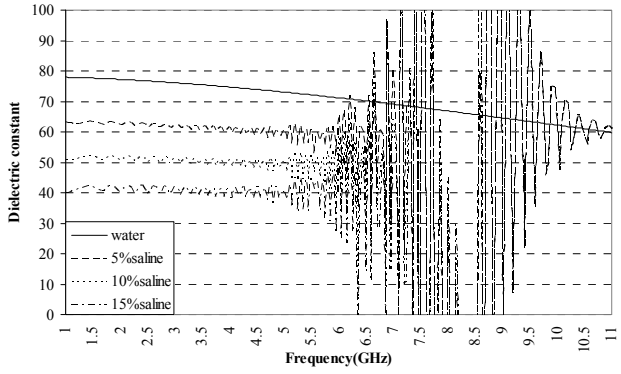

(a)

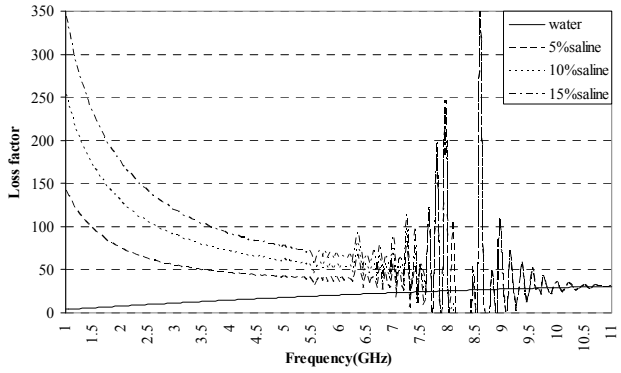

(b)

Fig. 6. Variation of dielectric properties of lower layer (d = 5 mm, W = 18λ at 6 GHz): (a) Dielectric constant, (b) Loss factor.

4. Experimental Results

4.1 Experimental Setup

A plastic container of 60 cm × 90 cm × 52 cm in size, which the aperture area is 0.54 m^2, was first filled with 5% saline solution until reaching 40 cm in depth from the bottom. A large plastic sheet (thickness of 0.1 mm) was laid over the surface of saline solution. Its edges are wrapped on the edges of the plastic container. A plastic sheet was pressed to delete air bubbles. This plastic sheet can be used as a flat separator between saline solution and water before water of thickness of 5 mm was filled on top of the plastic sheet. The temperatures of water and the 5% saline solution were 25 °C. This container was surrounded by wave absorbers, and two conical log antennas were used to transmit and receive microwave signal. The photograph of the measurement setup is depicted in Fig. 7. The frequency was varied from 1 GHz to 11 GHz, with the transmitting power of 10 mW using a vector network analyzer. The polarization of the transmitting and receiving antennas was respectively right-hand and left-hand circular polarization as these are the available wideband antennas in our laboratory. The antennas were separated by a wave absorber to decouple the antennas (measured S_{21} of –50 dB). The distance from the antennas to the surface of water was 1 m. It was calculated from the largest dimension of the antenna at the center frequency [25]. Note that this distance is shorter than the distance calculated from the largest dimension of the sample. Hence, the planar wavefront is not ensured. This may affect the accuracy of the upper layer thickness determination. A vector network analyzer was open, short and load calibrated and used for reflection measurement. The method to obtain a linear polarized wave from the circular polarized wave can be explained as follows:

$\vec{E}_{receive}$ is the received wave at the receiving antenna.

$$\begin{aligned}\vec{E}_{receive} &= \Gamma E_i \hat{a}_w \cdot \hat{a}_{ant} \\ &= \Gamma[E_x \hat{a}_x + jE_y \hat{a}_y] \cdot [\hat{a}_x \mp j\hat{a}_y] \end{aligned} \quad (16)$$

where Γ is the complex reflection coefficient of the object under test, E_i is incident electric wave, $\hat{a}_w$ is polarization vector of the incident wave, and $\hat{a}_{ant}$ is polarization vector of receiving antenna. When the transmitted right-hand circular polarized wave (RHCP) is received by a right-hand circular polarized antenna (RHCP), the received wave is

$$\Gamma[(E_x + E_y)]. \quad (17)$$

The wave received by the left-hand circular polarized antenna (LHCP) can be expressed by (16).

$$\Gamma[(E_x - E_y)]. \quad (18)$$

Therefore, the linear polarized wave can be found from (17) ± (18) and then divided by 2.

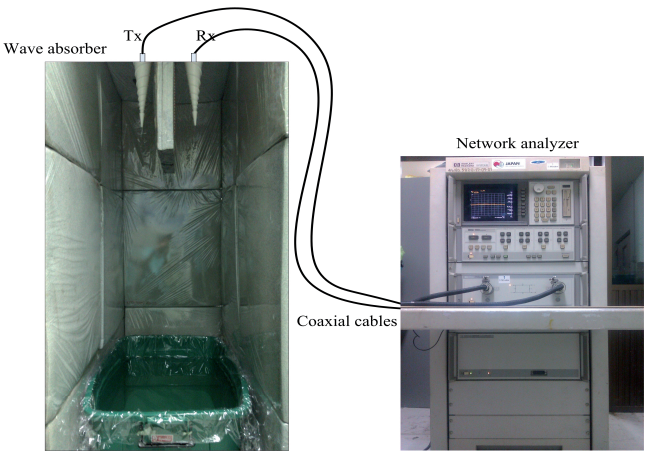

Fig. 7. Experimental setup.

Note that receiving the transmitted RHCP wave by a RHCP antenna corresponds to measuring S_{11} whereas receiving by LHCP antenna corresponds to measuring S_{21}.

This assumption is realizable since the RHCP and LHCP antennas are connected to ports 1 and 2 of the network analyzer, respectively. In addition, the reflected wave from the material under test is in the main beam direction of the antennas which polarization is almost purely circular polarization.

4.2 System Calibration

The system was calibrated by placing a conducting plate (made of copper with a thickness of 1.44 mm that does not contribute significantly to phase error) on the surface of water (see Fig. 8(a)). The total reflection coefficient (Γ_{total_PEC}) is the summation of mutual coupling (S_{21}) and reflection from the conducting plate which is assumed to be perfect conductor ($\Gamma_{in\_copper}=-1$). S_{21} can be determined from

$$S_{21} = \Gamma_{total\_PEC} - \Gamma_{in\_copper}. \tag{19}$$

After removing the conducting plate, the reflection coefficient of the material under test was measured as shown in Fig. 8(b). The total reflection coefficient is the summation of the mutual coupling of the antennas (S_{21}) and the reflection coefficient of water and saline solution interface. Substituting S_{21} in (19) one can find the reflection coefficient between saline solution and water as shown in (20).

$$\Gamma_{in\_water,5\%saline} = \\ = \Gamma_{total\_water,5\%saline} - \left(\Gamma_{total\_PEC} - \Gamma_{in\_copper}\right) \tag{20}$$

The calibrated-measured reflection coefficient can be found from the measured reflection coefficients from the material under test and the reflection of the conducting plate.

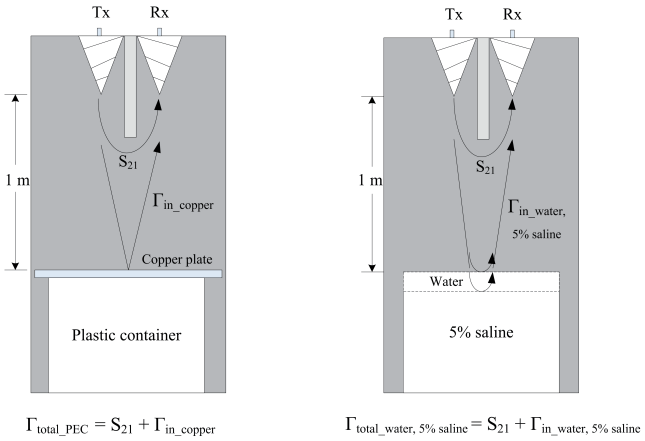

Fig. 8. Calibration process: (a) Conducting plate measurement. (b) Water and 5% saline solution measurement.

4.3 Experimental Results

The calibrated-measured results were substituted on the left side of (4b) and the dielectric constant and loss factor were determined from (12) and (13).

Fig. 9 shows of the measured dielectric properties. Figs. 9(a) and (b) are respectively for dielectric constant and loss factor when the water is 5 mm thick. Clearly, the dielectric properties approach those of water at frequencies higher than 10.7 GHz as the depth of penetration of the wave is shorter than the thickness of water.

The comparisons of the measured results show the error of thickness is in the order of 5.6%. The discrepancy can be attributed from residue transmission at the high frequency and the effect of a plastic sheet separating the two media. The error from the determined dielectric properties of the upper layer results in error in velocity of wave in the upper layer and hence the depth of the upper layer. Nevertheless, a good agreement of the determined dielectric constant can be accomplished with slight error. For the loss factor, the fluctuations around the actual values are attributed from the limited signal-to-noise ratio in the experiment. It is recommended to utilize sufficiently high signal-to-noise ratio in practical use.

Comparing the measured results in Fig. 9 to the calculation results in Fig. 4, the good agreement is obtained. The dielectric properties of the lower layer approach those of 5% saline. While those in Fig. 4 are obtained at fre-

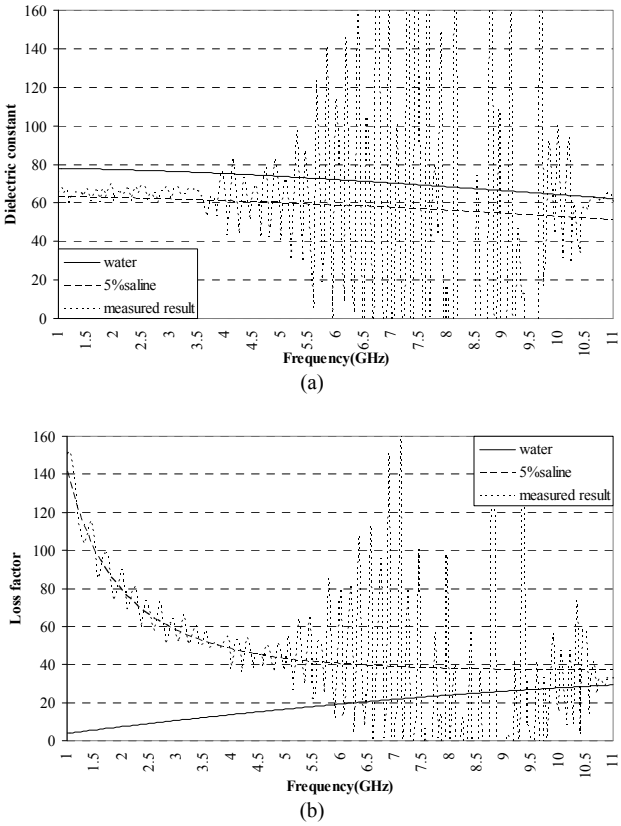

Fig. 9. Determined dielectric properties for $d = 5$ mm: (a) Dielectric constant. (b) Loss factor.

quency lower than 4.5 GHz, the results in Fig. 9 are obtained at frequency lower than 3.5 GHz. The difference results from the calculation results in Fig. 4 neglects the multiple reflections in the upper layer. In addition, the size of the measured material is not exactly the same as the one in calculation. Hence, the effect of edge diffraction is different.

5. Discussion

From the results in the previous sections, it is worth mentioning about the limitation of the system and the required bandwidth for the specific measurement.

The main objective of this work is to determine the unknown dielectric properties of the lower material at the lower frequency band. The upper material is the known material which is determined from the measured reflection coefficient at the higher frequency band. Then, from these dielectric properties at higher frequency band, the dielectric properties at lower frequency band can be found from the wideband database, which is already measured and cataloged as the priori data. With the dielectric properties at the lower frequency band, they lead to the determination of the dielectric properties of the lower material.

It is also essential to discuss about the required bandwidth of the measurement system. The bandwidth is directly related to the dielectric properties and thickness of the upper material. It is obtained from the inverse Fourier transform of the frequency domain measurement to time domain. Then, the thickness is obtained from (15). The thickness d contributes to the accuracy of the determined dielectric properties of the lower material, as seen in (7).

For the high loss material in the upper layer, the depth of penetration is shallow. For instance, when the upper layer is water the minimum d is 5 mm with error of 3.4%. For d less than 5 mm error is in excess of 10%. On the other hand, for the upper layer of 5% saline, the minimum d is 3 mm. The d thinner than 3 mm, error is excessively high. Hence, dielectric properties and thickness of the upper layer play a key role in the required bandwidth.

Furthermore, for the thick upper layer the required high frequency that wave does not penetrate to the lower layer decreases. For instance, for the same condition that the upper layer is water and the lower layer is 5% saline, the thicker upper layer requires lower frequency band. The system design for the measurement bandwidth can be accomplished by calculation using the proposed technique.

6. Conclusion

This paper has presented a dielectric properties determination technique for a stratified medium. The issue of interest in this work is a two-layer planar dielectric structure in which both the dielectric properties for the lower layer and the thickness of the upper layer are unknown. The reflection coefficients of both layers were derived and the dielectric constant and loss factor of the lower medium were extracted. The technique started with wideband measurement to obtain the frequency domain response. The steady response on high frequency exhibited the effect of only the upper layer since wave could not penetrate to the lower layer. Therefore, a single layer was considered at this frequency band and dielectric properties could be accurately determined. Then, the full band dielectric properties were utilized for determining the depth of penetration. The full band dielectric properties and the time domain response can be obtained from the inverse Fourier transform. Hence, the thickness of the upper layer was determined. Using the derived dielectric properties extraction expressions, the dielectric properties of the lower layer can be determined. The measured results in 1-11 GHz band using 5 mm-thick water and 5% saline solution validated the proposed technique at the frequency below 3.5 GHz. The good agreement is accomplished and the proposed technique can be applied for justifying material in industrial process.

Acknowledgements

This work was supported by Thailand Research Fund under the Royal Golden Jubilee Ph.D. Program, Grant no. PHD/0323/2551 and King Mongkut's Institute of Technology Ladkrabang Research Fund (Grant no. KREF115061). The authors faithfully appreciate Mr. Vichit Lohprapan for kindly proofreading the manuscript.

References

[1] GHODGAONKAR, D. K., VARADAN, V. V., VARADAN, V. K. A free-space method for measurement of dielectric constants and loss tangents at microwave frequencies. *IEEE Transactions on Instrumentation and Measurement,* 1989, vol. 37, no. 3, p. 789–793. DOI: 10.1109/19.32194

[2] ZOUGHI, R., BAKHTIARI, S. Microwave nondestructive detection and evaluation of disbounding and delamination in layered-dielectric-slabs. *IEEE Transaction on Instrumentation and Measurement,* 1990, vol. 39, no. 6, p. 1059–1063. DOI: 10.1109/19.65826

[3] VENKATESH, M. S., RAGHAVAN, G. S. V. An overview of dielectric properties measuring techniques. *Canadian Biosystems Engineering,* 2005, vol. 47, p. 7.15–7.30.

[4] SINGH, D., YAMAGUCHI, Y., YAMADA, H., SINGH, K. P. Response of microwave on bare soil moisture and surface roughness by X-band scatterometer. *IEICE Transactions on Communications,* 2000, vol. E83-B, no. 9, p. 2038–2043.

[5] KHARKOVSKY, S., AKAY, M. F., HASAR, U. C., ATIS, C. D. Measurement and monitoring of microwave reflection and transmission properties of cement-based specimens. *IEEE Transactions on Instrumentation and Measurement,* 2002, vol. 51, no. 6, p. 1210–1218. DOI: 10.1109/TIM.2002.808081

[6] THAKUR, K. P., HOLMES, W. S. Noncontact measurement of moisture in layered dielectrics from microwave reflection spectroscopy using an inverse technique. *IEEE Transactions on Microwave Theory and Techniques,* 2004, vol. 52, no. 1, p. 76–82. DOI: 10.1109/TMTT.2003.821243

[7] HASAR, U. C., WESTGAT, C. R., ERTUGRUL, M. Permittivity determination of liquid materials using waveguide measurements for industrial applications. *IET Microwave, Antennas and Propagation,* 2010, vol. 4, no. 1, p. 141–152. DOI:10.1049/iet-map.2008.0197

[8] MEHTA, P., CHAND, K., NARAYANSWAMY, D., BEETNER, D. G., ZOUGHI, R., STOECKER, W. V. Microwave reflectrometry as a novel diagnostic tool for detection of skin cancers. *IEEE Transactions on Instrumentation and Measurement,* 2006, vol. 55, no. 4, p. 1309–1316. DOI: 10.1109/TIM.2006.876566

[9] SEKIGUCHI, H., SHIRAI, H. Electromagnetic scattering analysis for crack depth estimation. *IEICE Transactions on Electronics,* 2003, vol. E86-C, no. 9, p. 2224–2229.

[10] GHASR, M. T., KHARKOVSKY S., ZOUGHI, R., AUSTIN, R. Comparison of near-field millimeter-wave probes for detecting corrosion precursor pitting under paint. *IEEE Transactions on Instrumentation and Measurement,* 2005, vol. 54, no. 4, p. 1497–1504. DOI: 10.1109/TIM.2005.851086

[11] GHASR, M. T., CARROL, B., KHARKOVSKY, S., AUSTIN, R., ZOUGHI, R. Millimeter-wave differential probe for nondestructive detection of corrosion precursor pitting. *IEEE Transactions on Instrumentation and Measurement,* 2006, vol. 55, no. 5, p. 1620–1627. DOI: 10.1109/TIM.2006.880273

[12] HUGHES, D., ZOUGHI, R. A novel method for determination of dielectric properties of materials using a combined embedded modulated scattering and near-field microwave techniques. Part I-Forward model. *IEEE Transactions on Instrumentation and Measurement,* 2005, vol. 54, no. 6, p. 2389–2397. DOI: 10.1109/TIM.2005.858132

[13] HUGHES, D., ZOUGHI, R. A novel method for determination of dielectric properties of materials using a combined embedded modulated scattering and near-field microwave techniques. Part II-Dielectric property recalculation. *IEEE Transactions on Instrumentation and Measurement,* 2005, vol. 54, no. 6, p. 2398-2401. DOI: 10.1109/TIM.2005.858133

[14] VENKATESH, M. S., RAGHAVAN, G. S. V. An overview of microwave processing and dielectric properties of agri-food materials. *Journal of Biosystems Engineering,* 2004, vol. 88, no. 1, p. 1–18. DOI: 10.1016/j.biosystemseng.2004.01.007

[15] NELSON, S. O. Agricultural applications of dielectric measurements. *IEEE Transactions on Dielectrics and Electrical Insulation,* 2006, vol. 13, no. 4, p. 688–702. DOI: 10.1109/TDEI.2006.1667726

[16] ABUDUL KHALID, M. F., RAMLI, A. S., BABA, N. H., SAAD, H. A novel preliminary study on microwave characterization of siamese mangoes ripeness at K-band. In *Proceedings of International RF and Microwave Conference.* Kuala Lumpur (Malaysia), 2008, p. 143–147.

[17] HASAR, U. C. A fast and accurate amplitude-only transmission-reflection method for complex permittivity determination of lossy materials. *IEEE Transactions on Microwave Theory and Techniques,* 2008, vol. 56, no. 9, p. 2129–2135. DOI: 10.1109/TMTT.2008.2002229

[18] ODA, M., MASE, A., UCHINO, K. Non-destructive measurement of sugar content in apples using millimeter wave reflectometry and artificial neural networks for calibration. In *Proceedings of the 25th Asia-Pacific Microwave Conference.* Melbourne (Australia), 2011, p. 1386–1389.

[19] GHASR, M. T., SIMMS, D., ZOUGHI, R. Multimodal solution for a waveguide radiating into multilayered structures-dielectric property and thickness evaluation. *IEEE Transactions on Instrumentation and Measurement,* 2009, vol. 58, no. 5, p. 1505–1513. DOI: 10.1109/TIM.2008.2009133

[20] SEAL, M. D., HYDE, M. W., HAVRILLA, M. J. Nondestructive complex permittivity and permeability extraction using a two-layer dual-waveguide probe measurement geometry. *Progress In Electromagnetics Research,* 2012, vol. 123, p. 123–142. DOI:10.2528/PIER11111108

[21] CHARVAT, G. L., KEMPEL, L. C., ROTHWELL, E. J., COLEMAN, C. M., MOKOLE, E. L. A through-dielectric radar imaging system. *IEEE Transactions on Antennas and Propagation,* 2010, vol. 58, no. 8, p. 2594–2603. DOI: 10.1109/TAP.2010.2050424

[22] OSA, K., SUMANTYO, J. T. S., NISHIO, F. An application of microwave measurement for complex dielectric constants to detecting snow and ice on road surface. *IEICE Transactions on Communications,* 2011, vol. E94-B, no. 11, p. 2987–2990. DOI: 10.1587/transcom.E94.B.2987

[23] GENNARELLI, G., RICCIO, G. A uniform asymptotic solution for the diffraction by a right-angle dielectric wedge. *IEEE Transactions on Antennas and Propagation*, 2011, vol. 59, no. 3, p. 898–903. DOI: 10.1109/TAP.2010.2103031

[24] STOGRYN, A. Equations for calculating the dielectric constant of saline water. *IEEE Transactions on Microwave Theory and Techniques,* 1971, vol. MTT-19, no. 8, p. 733–736. DOI: 10.1109/TMTT.1971.1127617

[25] KRAUS, J. D., MARHEFKA, R. J. *Antennas for All Applications*. 3rd ed. New York: McGraw-Hill, 2002.

About the Authors ...

Paiboon YOIYOD was born in Phetchaburi in 1981, Thailand. He received the Bachelors degree in Electrical Engineering with first class honor from Rangsit University and Masters degree in Telecommunications Engineering from King Mongkut's Institute of Technology Ladkrabang in 2005 and 2010, respectively. He is currently pursuing the Ph.D. degrees in Electrical Engineering. He joined in production engineer, Pioneer Manufacturing (Thailand) Co.,Ltd. in 2005 as an engineer. In 2006, he joined the Rangsit University as an engineer. His current research interests include dielectric measurements, sensors, and measurement systems.

Monai KRAIRIKSH was born in Bangkok, Thailand. He received the B.Eng., M.Eng. and D.Eng. degrees in Electrical Engineering from King Mongkut's Institute of Technology Ladkrabang (KMITL), Thailand in 1981, 1984, and 1994, respectively. He was a visiting research scholar at Tokai University in 1988 and at Yokosuka Radio Communications Research Center, Communications Research Laboratory (CRL) in 2004. He joined the KMITL and is currently a Professor at the Department of Telecommunication Engineering. He has served as the Director of the Research Center for Communications and Information Technology during 1997-2002. His main research interests are in antennas for mobile communications and microwave in agricultural applications. Dr. Krairiksh was the chairman of the IEEE MTT/AP/Ed joint chapter in 2005 and 2006. He served as the General Chairman of the 2007 Asia-Pacific Microwave Conference, and the advisory committee

of the 2009 International Symposium on Antennas and Propagation. He was the President of the Electrical Engineering/Electronics, Computer, Telecommunications and Information Technology Association (ECTI) in 2010 and 2011 and was an editor-in-chief of the ECTI Transactions on Electrical Engineering, Electronics, and Communications. He was recognized as a Senior Research Scholar of the Thailand Research Fund in 2005 and 2008 and a Distinguished Research Scholar of the National Research Council of Thailand. He has been a distinguished lecturer of IEEE Antennas and Propagation Society during 2012-2014.